J. Synchrotron Rad. (1998). **5**, 1130–1132

High-spatial-resolution and real-time medical imaging using a high-sensitivity HARPICON camera

Keiji Umetani,[a]*† Hironori Ueki,[a] Tohoru Takeda,[b] Yuji Itai,[b] Hidezo Mori,[c] Etsuro Tanaka,[c] Minhaz Uddin-Mohammed,[c] Yoshiro Shinozaki,[c] Masayoshi Akisada[d,e] and Yasuhito Sasaki[f,g]

[a]Central Research Laboratory, Hitachi Ltd, Kokubunji, Tokyo 185, Japan, [b]Institute of Clinical Medicine, University of Tsukuba, Tsukuba, Ibaraki 305, Japan, [c]Tokai University School of Medicine, Bohseidai Isehara, Kanagawa 259-11, Japan, [d]Tama Health Management Center, Tachikawa, Tokyo 190, Japan, [e]Department of Radiology and Information Science, International University of Health and Welfare, Ohtawara, Tochigi 324, Japan, [f]Faculty of Medicine, University of Tokyo, Bunkyo-ku, Tokyo 113, Japan, and [g]National Institute of Radiological Sciences, Inage-ku, Chiba 263, Japan. E-mail: umetani@spring8.or.jp

(*Received 4 August 1997; accepted 2 February 1998*)

A HARPICON™ camera has been applied to a digital angiography system with fluorescent-screen optical-lens coupling. It uses avalanche multiplication in the photoconductive layer for high-sensitivity imaging. The limiting spatial resolutions in the 1050 scanning-line mode of the camera are about 30 and 50 μm at input field sizes of 20 × 20 and 50 × 50 mm on the screen, respectively. For high-speed imaging, the 525 scanning-line mode at a rate of 60 images s^{-1} can be selected. High-quality images of coronary arteries in dogs were obtained by intra-aortic coronary angiography and superselective coronary angiography using a single-energy X-ray above the iodine *K*-edge energy.

Keywords: coronary angiography; aortography; micro-angiography; HARPICON camera.

1. Introduction

Coronary arterial disease is common in all industrial countries and can result in fatal heart attacks. The conventional method for diagnosing this disease is selective coronary angiography, which requires direct coronary arterial catheterization. As a safer and more repeatable method, dual-energy iodine *K*-edge transvenous coronary angiography using synchrotron radiation has been under investigation since the end of the 1970s (Rubenstein *et al.*, 1981). The dual-energy imaging systems have been improved for human studies by American and German research teams (Thomlinson, 1994; Thompson *et al.*, 1994; Dix *et al.*, 1994). On the other hand, a two-dimensional real-time imaging system with a single-energy approach has been investigated using monochromated X-rays just above the iodine *K*-edge energy (Takeda *et al.*, 1995; Ohtsuka *et al.*, 1997). The first human studies of transvenous coronary angiography using this approach were performed in Japan in May 1996.

We developed the dual-energy iodine *K*-edge transvenous coronary angiography system using an iodine filter method and could obtain real-time images of coronary arteries in a dog's heart (Umetani *et al.*, 1993). Though transvenous coronary angiography is less invasive than conventional selective coronary angiography, the image contrast is much lower than that of the conventional method because the contrast material is highly diluted and the circumflex artery of the left coronary artery is not shown because of overlap with opacified cardiac chambers. We have investigated an aortographic approach to overcome these problems using a high-spatial-resolution imaging system (Umetani *et al.*, 1996; Takeda *et al.*, 1997). The aortographic approach, in which a catheter is inserted into the aorta and its tip is placed near the aortic valve, is more invasive than transvenous coronary angiography but is less invasive than conventional selective coronary angiography. We have also evaluated a superselective coronary angiographic approach in which a catheter with a small diameter is inserted into the coronary artery to place its tip in an epicardial branch artery of the coronary artery to observe blood flow in the penetrating transmural arteries (Mori *et al.*, 1996).

2. Imaging method

The X-ray imaging system shown in Fig. 1 was placed at beamline BL-14C at the Photon Factory, Tsukuba, Japan (Umetani *et al.*, 1996). The synchrotron radiation beam is monochromated and expanded horizontally by an asymmetrically cut silicon ⟨311⟩ crystal for two-dimensional imaging. X-rays are transformed into a visible image by a fluorescent screen. Images with dimensions of 20 × 20 and 50 × 50 mm on the screen are read by a HARPICON camera that has two sets of lenses with a high numerical aperture of *f*/0.65. The demagnification factors of these sets of lenses are 1.6:1 for 20 mm images and 4:1 for 50 mm. The screens use a gadolinium oxysulfide phosphor with a phosphor layer thicknesses of 90 μm for 20 mm images and 115 μm for 50 mm. The HARPICON is a pickup tube with an amorphous selenium photoconductive target and is characterized by its internal amplification system, which uses stable avalanche multiplication of photo-generated carriers under a strong electric field in the photoconductive layer (Tsuji *et al.*, 1991). The medical-imaging HARPICON camera that we developed is 32 times more sensitive than conventional pickup-tube cameras.

Image signals from the camera are converted into digital format by an analog-to-digital converter with 12 bit resolution. Real-time images are stored in a frame memory at a rate of 15 and 60 images s^{-1} with image formats of 1024 × 960 and 512 × 480 pixels corresponding to the camera's 1050 and 525 scanning-line modes, respectively. The equivalent pixel sizes projected onto the

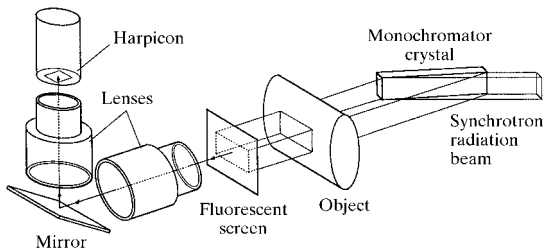

Figure 1
Schematic drawing of imaging system.

† Present address: Japan Synchrotron Radiation Research Institute (JASRI), SPring-8, Mikazuki-cho, Sayo-gun, Hyogo 679-5198, Japan.

screen area are about 20 and 50 μm in the 1050 scanning-line mode at input field sizes of 20 × 20 and 50 × 50 mm, respectively. In the 525 line mode, the equivalent pixel sizes are about 40 and 100 μm at field sizes of 20 and 50 mm, respectively.

3. Experiment and results

An X-ray image of the star chart in Fig. 2 was obtained in the highest spatial-resolution mode with the format of 1024 pixels at a field size of 20 mm. A spatial resolution of about 30 μm (16 line pairs mm^{-1}), which is the width of the narrowest parts of the tapered bar pattern around the center of the chart, could be imaged. However, the resolution of about 30 μm is less detailed than that defined by the equivalent pixel size of 20 μm because of resolution limitation caused by the fluorescent screen with a thickness of 90 μm. On the other hand, limiting spatial resolutions in the other three imaging modes are the same as those defined by the equivalent pixel sizes.

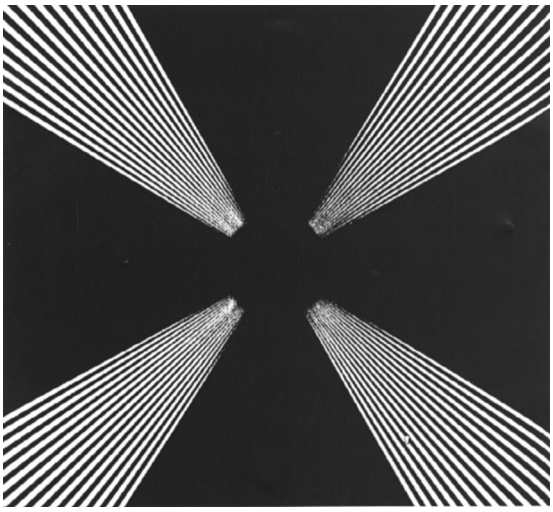

Figure 2
X-ray image of the spatial resolution chart.

In vivo imaging of intra-arterial injection angiography was performed in dogs weighing about 12 kg. X-ray energy was adjusted to 33.3 keV for single-energy imaging. The X-ray flux was around 8×10^8 photons mm^{-2} s^{-1} on the object surface.

For intra-aortic coronary angiography, a dog was anesthetized and a catheter was inserted into the aorta *via* the right femoral artery. Contrast material (12 ml) was injected at a rate of 12 ml s^{-1}. The aortographic image shown in Fig. 3 was obtained with the format of 512 pixels at a field size of 50 mm and a spatial resolution of 100 μm. The injected contrast material filled the aorta and coronary arteries and soon washed out of the aorta. As Fig. 3 shows, the main coronary arteries such as the left anterior descending coronary artery (LAD), the left circumflex coronary artery (LCX) and the right coronary artery (RCA) and their branches could be imaged clearly. The diameter of the LAD is less than 2 mm. The present experiment was approved by the Medical Committee for the Use of Animals in Research of the University of Tsukuba, and it conforms to the guidelines of the American Physiological Society.

Next, the preliminary experiment for superselective coronary angiography was performed. Penetrating transmural arteries are considered to be a critical vascular component that causes a transmural variation of myocardial blood flow under various pathophysiological conditions. This imaging system has potential as a diagnostic tool for circulatory disorders in small vessels. In the preliminary experiment, another dog was anesthetized and a silicon-tube bypass graft was placed between the subclavian artery and the epicardial branch of the left anterior descending coronary artery. Contrast material (5 ml) was injected into the bypass graft

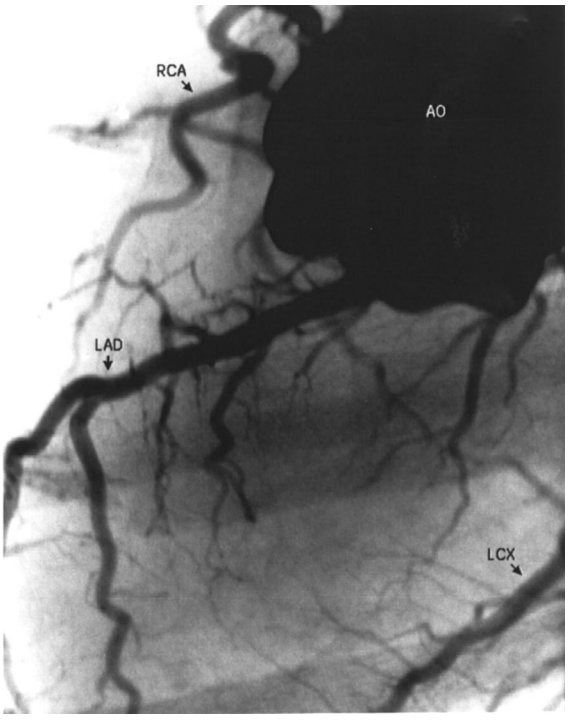

Figure 3
Aortographic image of a dog showing the left anterior descending coronary artery (LAD), the left circumflex coronary artery (LCX), the right coronary artery (RCA) and the aorta (AO).

Figure 4
Superselective coronary angiographic image of a dog showing the penetrating transmural coronary arteries (white arrows) originating in the terminal segments of the epicardial coronary arteries (black arrows).

at a rate of 3 ml s^{-1} and real-time images were taken with the format of 512 pixels at a field size of 20 mm and a spatial resolution of 40 μm. As Fig. 4 shows, the penetrating transmural arteries originate in the terminal segments of the epicardial coronary arteries (the left anterior descending coronary artery and the diagonal branch) and penetrate toward the left ventricular cavity through the heart wall. The diameters of the penetrating transmural arteries are around 100 μm. The present experiment was performed in accordance with the Guidelines of Tokai University School of Medicine on Animal Use, which conform to the guidelines of the US National Institutes of Health.

4. Concluding remarks

A HARPICON camera has been applied to X-ray medical imaging using a fluorescent-screen lens-coupling approach. The imaging system was capable of a spatial resolution of about 30 μm in the highest spatial-resolution mode. In intra-aortic coronary angiography in the 100 μm-resolution mode, the dog's heart image is believed to be sufficient for clinical diagnosis because of clear coronary artery structures. The aortographic procedure is much safer and more easily repeatable than conventional selective coronary angiography. This result indicates that screening of coronary arterial disease can be performed safely and repeatably by using this method. In the preliminary experiment for superselective coronary angiography with the 40 μm-resolution mode, real-time images of the penetrating transmural arteries with a diameter of around 100 μm were obtained. The images demonstrate the usefulness of the real-time micro-angiography system for the identification of circulatory disorders in small vessels.

The authors thank Dr Osamu Shimomura of the Photon Factory for support in experiments at BL-14C. This work was performed with the approval of the National Laboratory for High Energy Physics (acceptance No. 95-Y005) and the Photon Factory Program Advisory Committee (proposal Nos. 95-G290 and 95-G113).

References

Dix, W. R., Graeff, W., Hamm, C., Heuer, J., Hultschig, H., Kupper, W., Lohmann, M. & Rust, C. (1994). *Synchrotron Radiation in the Biosciences*, edited by B. Chance, J. Deisenhofer, S. Ebashi, D. T. Goodhead, J. R. Helliwell, H. E. Huxley, T. Iizuka, J. Kirz, T. Mitsui, E. Rubenstein, N. Sakabe, T. Sasaki, G. Schmahl, H. B., Stuhrmann, K. Wüthrich & G. Zaccai, pp. 666–673. Oxford University Press.

Mori, H., Hyodo, K., Tanaka, E., Uddin-Mohammed, M., Yamakawa, A., Shinozaki, Y., Nakazawa, H., Tanaka, Y., Sekka., T., Iwata, Y., Handa, S., Umetani, K., Ueki, H., Yokoyama, T., Tanioka, K., Kubota, M., Hosaka, H., Ishikawa, N. & Ando, M. (1996). *Radiology*, **201**, 173–177.

Ohtsuka, S., Sugishita, Y., Takeda, T., Itai, Y., Hyodo, K. & Ando, M. (1997). *Jpn. Circ. J.* **61**, 432–440.

Rubenstein, E., Hughes, E. B., Campbell, L. E., Hofstadter, R., Kirk, R. L., Krolicki, T. J., Stone, J. P., Wilson, S., Zeman, H. D., Brody, W. R., Macovski, A. & Thompson, A. C. (1981). *SPIE Proc.* **314**, 42–49.

Takeda, T., Itai, Y., Wu, J., Ohtsuka, S., Hyodo, K., Ando, M., Nishimura, K., Hasegawa, S., Akatsuka, T. & Akisada, M. (1995). *Acad. Radiol.* **2**, 602–608.

Takeda, T., Umetani, K., Doi, T., Echigo, J., Ueki, H., Ueda, K. & Itai, Y. (1997). *Acad. Radiol.* **4**, 438–445.

Thomlinson, W. (1994). *Synchrotron Radiation in the Biosciences*, edited by B. Chance, J. Deisenhofer, S. Ebashi, D. T. Goodhead, J. R. Hellwell, H. E. Huxley, T. Iizuka, J. Kirz, T. Mitsui, E. Rubenstein, N. Sakabe, T. Sasaki, G. Schmahl, H. B., Stuhrmann, K. Wüthrich & G. Zaccai, pp. 674–680. Oxford University Press.

Thompson, A. C., Lavender, W. M., Chapman, D., Gmur, N., Thomlinson, W., Rosso, V., Schulze, C., Rubenstein, E., Giacomini, J. C., Gordon, H. J. & Dervan, J. P. (1994). *Nucl. Instrum. Methods*, A**347**, 545–552.

Tsuji, K., Ohshima, T., Hirai, T., Gotoh, N., Tanioka, K. & Shidara, K. (1991). *Mater. Res. Soc. Symp. Proc.* **219**, 507–518.

Umetani, K., Ueda, K., Takeda, T., Itai, Y., Akisada, M. & Nakajima, T. (1993). *Nucl. Instrum. Methods*, A**335**, 569–579.

Umetani, K., Ueki, H., Ueda, K., Hirai, T., Takeda, T., Doi, T., Wu, J., Itai, Y. & Akisada, M. (1996). *J. Synchrotron Rad.* **3**, 136–144.